

Non-hermitean delocalization in an array of wells with variable-range widths

V.G.Benza

Facolta' di Scienze, Universita' dell'Insubria
Via Lucini 3, 22100 Como
also INFN, unita' di Milano,
Via Celoria 16, 20133 Milano

November 13, 2018

Abstract

Nonhermitean hamiltonians of convection-diffusion type occur in the description of vortex motion in the presence of a tilted magnetic field as well as in models of driven population dynamics. We study such hamiltonians in the case of rectangular barriers of variable size. We determine Lyapunov exponent and wavenumber of the eigenfunctions within an adiabatic approach, allowing to reduce the original $d=2$ phase space to a $d=1$ attractor.

PACS numbers:05.70.Ln,72.15Rn,74.60.Ge

1 Introduction

Quantum mechanics in an imaginary magnetic field (IMF) has been studied by various authors, after Hatano and Nelson [1] pointed out its relevance in describing the competition between drift and pinning for a vortex in the presence of columnar defects. The kinetic part of the hamiltonian with IMF is a convection-diffusion operator; operators of this type occur as well in models of driven population dynamics [2], [3], [4]. Due to the convection term, parity is violated and the wave function is exponentially magnified along a given direction; as a consequence, it can keep a localized character provided its decay, generated by the disordered potential, wins over the IMF amplification.

In the zero-IMF reference hamiltonian the decay, if disorder does not violate parity, is characterized by the inverse of a single localization length on both sides. With convection, when the decay is exactly compensated by the IMF magnification factor, the wave function becomes delocalized. The spectrum at the critical point bifurcates, and is distributed along a $d=1$ curve in the complex plane. This scenario was proved to be valid with various potential distributions (gaussian, box, Cauchy); it has been confirmed for lattice models with disordered hopping [5],[6], [7], [8], [9], [10].

In the hermitean case, one can turn the eigenvalue problem into a Langevin equation, and determine the spectral properties [11] from the steady state distribution of the Langevin problem.

Here we generalize this approach to complex-valued stochastic equations, as needed when dealing with non-hermitean hamiltonians. Rather than starting with a gaussian δ -correlated potential, which would lead to a Langevin equation, we consider a piecewise constant potential $V(x)$, a model originally studied by Benderskii and Pastur [12] in the hermitean case. The reasons for our choice will become clear in the sequel. If, e.g., $V(x) = V_0, V_1$ with $V_0 = 0$ and $V_1 < 0$, $V(x)$ describes equally engineered trapping defects in an homogeneous medium.

We assume that free segments and trapping segments are independent random variables, with fixed average length l_0, l_1 respectively. Although the stochastic equation is no longer of Langevin type, the probability distribution still satisfies a differential equation. This equation allows for an adiabatic approach, which would be impossible with white noise. We can thus reduce the phase space to a one-dimensional attractor \mathcal{L} , strongly simplifying the search for steady state.

The “dynamic variable” of the stochastic equation is the logarithmic derivative $z(x)$ of the wave function. From the mean value $\langle z(E) \rangle$, ($E = E_r + i \cdot E_i$) one extracts the inverse of the localization length, as well as a wavenumber. Generically we find that the localization length decreases when E departs from the real axis, and increases with E_r .

This behavior implies that, in the presence of an IMF, at a critical value of E_r the system delocalizes; the contour lines of $\langle z_r(E) \rangle$ determine then the mobility edge in the complex energy plane. Three different regimes (low, high and intermediate E_r) will be analyzed in the next three sections.

2 Langevin formulation of the quantum eigenvalue problem

The eigenvalue problem $\hat{H}\psi = E \cdot \psi$ for a d=1 Hamiltonian $\hat{H}_0 = -\frac{d^2}{dx^2} + V(x)$ with disordered potential $V(x)$ translates into a Langevin equation for the logarithmic derivative z of the wave function ψ :

$$\frac{dz}{dx} = -(z^2 + E) + V(x); \quad z = \frac{\psi'}{\psi}. \quad (1)$$

As is well known, one can limit the analysis to real-valued wave functions. The deterministic part of the equation is invariant under space inversion ($z(-x) = -z(x)$) ; hence, if the statistical properties of $V(x)$ are also invariant, the backward and forward x -evolution of z are equivalent, i.e. they approach the same steady state. One defines the Lyapunov exponent $\gamma(E)$:

$$\begin{aligned} \gamma(E) &= \lim_{x \rightarrow \infty} \frac{\langle \ln r(x) \rangle}{x} \\ r^2(x) &= \psi^2(x) + \psi'^2(x) \end{aligned}$$

where the average is over $V(x)$; $\gamma(E)$ is always positive for disordered potentials with rapidly decaying correlations [14]. The following identity is shown to hold:

$$\gamma(E) = \langle z \rangle \quad (2)$$

The Lyapunov exponent is an index for the exponential growth rate of the wave function ($\psi(x) \approx \exp[\pm\gamma \cdot x]$ $x \rightarrow +\infty$): here, by Oseledec's theorem, the plus sign always occurs, but for a single case, corresponding to the physical (square-summable) solution [13]. Consistently, one has indeed $\langle z \rangle > 0$ and a non-even steady state distribution $P(z)$.

Let us now examine how this picture is changed upon adding an external (constant) imaginary magnetic field (IMF). In the hamiltonian, this is mimicked by: $\hat{H} = -(\frac{d}{dx} - a)^2 + V(x)$, implying $z \rightarrow z - a$ in Eq. 1, which now is to be studied for complex z and E ($z = z_r + i \cdot z_i$, $E = E_r + i \cdot E_i$). The space-inversion invariance is broken by the convection term $a \cdot \frac{d}{dx}$ and different exponential growth rates are found at $x \rightarrow +\infty$ and $x \rightarrow -\infty$. On qualitative grounds, the asymptotic behavior is $\psi(\pm L) \approx \exp[(\pm \cdot a - \langle z_r(E) \rangle) \cdot L]$ ($L \gg 1$) and delocalization occurs when $\langle z_r(E) \rangle - a = 0$.

If one gauges away the IMF from the Schrodinger equation, Eq. 1 is restored, but the boundary conditions are changed: e.g., in the case of a double-sided problem, from $\psi(-L) = \alpha_-$, $\psi(L) = \alpha_+$, one has $\psi(-L) = \exp(a \cdot L) \cdot \alpha_-$, $\psi(L) = \exp(-a \cdot L) \cdot \alpha_+$.

We are not going to study the spectrum, but rather the vanishing of the "effective" Lyapunov exponent $\langle z_r(E) \rangle - a$. In order to do that it is sufficient to study the steady state distribution $P(z) = P(z_r, z_i)$ of Eq. 1 with $a = 0$, obtain $\langle z(E) \rangle$ and from it the contour lines of $\langle z_r(E) \rangle$. Notice that from the analysis a new object emerges, $\langle z_i(E) \rangle$, a sort of wavenumber of delocalized solutions.

In the search for steady state, we adopt an adiabatic approach. This is possible with our model potential, due to a property of Eq. 1 with $V(x) = 0$. Let us discuss this property first.

Equation 1 has two time-independent solutions (respectively stable and unstable critical point). If we denote with $\epsilon = \epsilon_r + i \cdot \epsilon_i$ one of the square roots of E , the critical points are $z_s = \epsilon_i - i \cdot \epsilon_r$ and $z_u = -\epsilon_i + i \cdot \epsilon_r$, (the suffixes s, u meaning stable and unstable respectively, with $\epsilon_i > 0$). It is easily verified that the Equation can be explicitly solved, for arbitrary initial conditions. After some algebra one obtains the announced property: the solutions satisfy an exact relation of the form:

$$\begin{aligned} \frac{|z(x)|^2}{|\epsilon|^2} &= \frac{\cosh(2B) - \cos(2A)}{\cosh(2B) + \cos(2A)} \\ A &= \epsilon_r \cdot (x - x_0) + \gamma_r \\ B &= \epsilon_i \cdot (x - x_0) + \gamma_i \end{aligned} \quad (3)$$

where γ_r and γ_i and x_0 are constants.

As a model potential, we take $V(x)$ two-valued, piecewise constant, $V(x) = (V_0, V_1)$. The lengths of the V_l intervals are two independent random variables with distributions $Q_l(x) = \frac{1}{c_l} \cdot \exp(-c_l \cdot x)$, ($l = \frac{1}{c_l}$).

In order to write the analog of Equation 1, we first introduce an independent stochastic variable $s(x)$, which assumes the values 0, 1 with distributions $Q_0(x)$, $Q_1(x)$.

The probability $P_0(x)$, $P_1(x)$ of $s(x)$ satisfies the rate equation:

$$\begin{aligned}\frac{dP_0}{dx} &= c_1 \cdot P_1 - c_0 \cdot P_0 \\ \frac{dP_1}{dx} &= c_0 \cdot P_0 - c_1 \cdot P_1,\end{aligned}\tag{4}$$

since $s(x)$ stays on the l -th channel an average “time” $\frac{1}{c_l}$.

The equation we looked for is then:

$$\frac{dz}{dx} = -(z^2 + E) + V_0 + s(x) \cdot (V_1 - V_0),\tag{5}$$

and, in components:

$$\begin{aligned}\frac{dz_r}{dx} &= -z_r^2 + z_i^2 - E_r + V_0 + s(x) \cdot (V_1 - V_0) \\ \frac{dz_i}{dx} &= -2 \cdot z_r \cdot z_i - E_i\end{aligned}\tag{6}$$

As is well known, from Eq.1, if $V(x)$ is gaussian, one gets a Fokker-Plank equation for the probability. Equation 5 is no longer of Langevin type, but one can show that the probability distribution still satisfies a differential equation. The details of the derivation can be found in Ref. [14] and in the original paper [12]. In terms of the probability $P(s, z; x) = P_0(z, x), P_1(z, x)$; ($P_0(z; x) = P(s = 0, z; x)$, $P_1(z; x) = P(s = 1, z; x)$) one has:

$$\begin{aligned}\frac{dP_0}{dx} &= \left(-\frac{d}{dz_r} F_r^{(0)} - \frac{d}{dz_i} F_i^{(0)}\right) P_0 + c_1 \cdot P_1 - c_0 \cdot P_0 \\ \frac{dP_1}{dx} &= \left(-\frac{d}{dz_r} F_r^{(1)} - \frac{d}{dz_i} F_i^{(1)}\right) P_1 - c_1 \cdot P_1 + c_0 \cdot P_0 \\ F_r^{(0)} &= -z_r^2 + z_i^2 - E_r + V_0 \\ F_r^{(1)} &= -z_r^2 + z_i^2 - E_r + V_1 \\ F_i^{(0)} &= F_i^{(1)} = -2 \cdot z_r \cdot z_i - E_i\end{aligned}\tag{7}$$

We finally state our adiabatic approximation. We assume that the coefficients c_0 and c_1 are very small with respect to the characteristic “frequencies” of the two deterministic evolutions $z^{(0)}(x)$ and $z^{(1)}(x)$, respectively associated with $E^{(0)} = E_r - V_0 + i \cdot E_i$ and $E^{(1)} = E_r - V_1 + i \cdot E_i$. Such frequencies, as one easily realizes, are the square roots $\epsilon^{(0)}$, $\epsilon^{(1)}$ of $E^{(0)}$ and $E^{(1)}$.

3 Low energy case

Let us examine the low E_r case. In both deterministic systems we assume $|\epsilon_r| < |\epsilon_i|$. This regime is out of the physical region since it implies $E_r < V_l$, ($l = 0, 1$); in spite of that, its analysis will be found to be useful in the sequel.

Upon averaging Eq. 3 over the variable B, which is fast varying with respect to A when $|\epsilon_r| < |\epsilon_i|$, the factor $\frac{\cosh(2B) - \cos(2A)}{\cosh(2B) + \cos(2A)}$ reduces to unity, and we obtain:

$$|z^{(l)}|^2 = |\epsilon^{(l)}|^2, \quad (l = 0, 1) \quad (8)$$

Each channel has a (metastable) attractor of circular shape, and the stochastic motion reduces to hops between such concentric orbits. The single channel deterministic dynamics is illustrated in Figs.1 and 2, where we show the vector field and the probability distribution for Eq. 5 when $s(x)$ is kept constant.

We now proceed to determine the steady state of Eq. 7. We first eliminate the z_i -dependence from $F_r^{(0)}$ and $F_r^{(1)}$ by means of Eq. 8, then average over z_i , and obtain:

$$\begin{aligned} \frac{d}{dz_r}(-2 \cdot z_r^2 + 2 \cdot (\epsilon_i^{(0)})^2)P_0 &= c_1 \cdot P_1 - c_0 \cdot P_0 \\ \frac{d}{dz_r}(-2 \cdot z_r^2 + 2 \cdot (\epsilon_i^{(1)})^2)P_1 &= -c_1 \cdot P_1 + c_0 \cdot P_0. \end{aligned} \quad (9)$$

Here $P_0 = P_0(z_r)$ and $P_1 = P_1(z_r)$, are averaged over z_i . The sum of the two equations gives:

$$(2 \cdot z_r^2 - 2 \cdot (\epsilon_i^{(0)})^2)P_0 + (2 \cdot z_r^2 - 2 \cdot (\epsilon_i^{(1)})^2)P_1 = K, \quad (10)$$

where K is a constant.

It is readily verified that only with $K = 0$ the positivity of the P 's is preserved. When $|z_r|$ is large enough the flow is in the negative z_r direction on both channels; it turns positive for $|z_r| < |\epsilon_i^{(l)}|$ ($l = 0, 1$) respectively.

Let us assume, without loss of generality, $0 < \epsilon_i^{(1)} < \epsilon_i^{(0)}$. A simple inspection of the hopping between channels shows that the particle gets trapped in the interval $\epsilon_i^{(1)} < z_r < \epsilon_i^{(0)}$; the probability is zero outside. Notice that upon including an indeterminacy in the radii of the two circular attractors we would get a non zero probability flow.

Apart from the normalization factor H , the solutions have the form:

$$\begin{aligned} P_0(z_r) &= H^{-1} \frac{1}{|z_r^2 - (\epsilon_i^{(0)})^2|} \cdot \psi(z_r) \\ P_1(z_r) &= H^{-1} \frac{1}{|z_r^2 - (\epsilon_i^{(1)})^2|} \cdot \psi(z_r) \\ \psi(z_r) &= \left[\left| \frac{z_r - \epsilon_i^{(0)}}{z_r - \epsilon_i^{(0)}} \right| \right]^{\mu_0} \cdot \left[\left| \frac{z_r - \epsilon_i^{(1)}}{z_r - \epsilon_i^{(1)}} \right| \right]^{\mu_1} \\ \mu_l &= \frac{c_l}{4 \cdot \epsilon_i^{(l)}} \end{aligned} \quad (11)$$

The function P_l has an integrable power law singularity at the l -th channel's stable point, and a zero at the opposite channel's stable point. If we denote with p_0 and p_1 the integrals of $P_0(z_r)$ and $P_1(z_r)$, they must satisfy the global equilibrium condition:

$$c_0 \cdot p_0 = c_1 \cdot p_1. \quad (12)$$

We determined the solution in the region $c_0 + c_1 = 1$ under this condition. The power exponent of the distribution is a function of the ratio $\frac{c_0}{c_1}$, i.e. it is shaped by the average “residence times” over the two channels. The mean value $\langle z_r \rangle$ is increasing with the ratio $\rho = \frac{\epsilon_i^{(0)}}{\epsilon_i^{(1)}}$, as shown in Fig.5. Since larger ratios imply larger values of $|V_0 - V_1|$, this simply means that the Lyapunov exponent increases with disorder, as it should be.

Any boundary condition $z_r(L) = \overline{z_L}$ with $\overline{z_L}$ lying outside the interval $\epsilon_i^{(1)} < z_r < \epsilon_i^{(0)}$ cannot be fulfilled: the density of states must then be zero in this regime, as anticipated.

4 High energy case

We analyze now the regime $E_r \gg 0$, which corresponds to the condition $|\epsilon_i| < |\epsilon_r|$ for both channels. To simplify the notation, unless when strictly necessary, in the next formulas we drop the channel index (l). Contrary to the former case, in Eq. 3 the variable A is now fast varying with respect to B. The average over A gives:

$$\frac{|z|^2}{|\epsilon|^2} = -1 + \frac{|z|^2 + |\epsilon|^2}{|\epsilon_r \cdot z_i - \epsilon_i \cdot z_r|}, \quad (13)$$

from which:

$$|\epsilon|^2 = |\epsilon_r \cdot z_i - \epsilon_i \cdot z_r|. \quad (14)$$

In a single channel, the metastable attractor is a couple of parallel lines: one through the stable, the other through the unstable critical point. Furthermore, the lines are orthogonal to the segment connecting such points. It appears that, in going from the low to the high energy limit, the attractor undergoes dilatation in the direction of such lines. This effect can already be seen in Fig.2, referring to the low energy regime.

An indeterminacy arises, about the line currently occupied by the “particle”:

$$z_i = \frac{\epsilon_i}{\epsilon_r} \cdot z_r \pm \frac{|\epsilon|^2}{\epsilon_r} \quad (15)$$

The single channel situation is illustrated in Figs.3 and 4, where we display the vector field and the probability distribution for Eq. 5 in the deterministic case.

The stochastic motion involves the union of two couples of parallel lines, with distinct slopes. We proceed with our strategy, based on averaging Eq. 7 over z_i . Upon writing $F_r^{(l)}$ ($l = 0, 1$) by means of Eq. 15 we have:

$$F_r = -z_r^2 + \left(\frac{\epsilon_i}{\epsilon_r} \cdot z_r\right)^2 \pm 2 \cdot \epsilon_i \cdot z_r + (\epsilon_i)^2, \quad (16)$$

where the dependence on E and V_l is written in terms of ϵ and the following approximation is made:

$$z_i = \frac{\epsilon_i}{\epsilon_r} \cdot z_r \pm \left(\epsilon_r + \frac{(\epsilon_i)^2}{\epsilon_r}\right) \approx \frac{\epsilon_i}{\epsilon_r} \cdot z_r \pm \epsilon_r. \quad (17)$$

The force $F^{(l)}(z_r)$ ($l = 0, 1$) acquires a fluctuating term, originated in the indeterminacy of Eq. 15; the term is of the order $2 \cdot \epsilon_i^{(l)} \cdot z_r$. The dynamics associated with this force has the form:

$$\frac{dz_r}{dx} = -z_r^2 + \left(\frac{\epsilon_i}{\epsilon_r} \cdot z_r\right)^2 + (\epsilon_i)^2 + 2 \cdot \epsilon_i \cdot z_r \cdot \eta(x), \quad (18)$$

where $\eta(x)$ is a white noise.

In summary, the mentioned indeterminacy adds to the stochasticity of the hopping between channels $l = 0, 1$; the process is then described by the Fokker-Plank equation:

$$\begin{aligned} \frac{dP_0}{dx} &= \frac{d}{dz_r}(-A^{(0)} + \frac{d}{dz_r}B^{(0)})P_0 + c_1 \cdot P_1 - c_0 \cdot P_0 \\ \frac{dP_1}{dx} &= \frac{d}{dz_r}(-A^{(1)} + \frac{d}{dz_r}B^{(1)})P_1 - c_1 \cdot P_1 + c_0 \cdot P_0 \\ A^{(l)} &= -(\alpha_l \cdot z_r)^2 + (\epsilon_i^{(l)})^2 \\ B^{(l)} &= D \cdot (\epsilon_i^{(l)})^2 \cdot [(z_r)^2 + (\xi^{(l)})^2] \\ \alpha_l^2 &= 1 - \left(\frac{\epsilon_i}{\epsilon_r}\right)^2 \end{aligned} \quad (19)$$

where D is the white noise coefficient and $\xi^{(l)}$ is a regularizing parameter (the criteria used in fixing this parameter are illustrated in the caption of Fig.6).

We evaluated numerically, by a perturbative procedure, the steady state solution of Eq. 19. To simplify things, we assumed $c_0 = c_1 = c < 1$. When the channels are uncoupled ($c = 0$), the problem can be explicitly solved along the lines of the hermitean case (see, e.g., Ref. [11]). The two equations reduce to the form: $\mathcal{M}^{(l)}P_l = \frac{d}{dz_r}J_l(z_r) = 0$, where, with obvious notation, $\mathcal{M}^{(l)}$ is the second order operator acting on P_l .

The solutions correspond to a constant probability current J_l and here look like:

$$\begin{aligned} P_l(z_r) &= \frac{J_l}{B_l(z_r)} \int_{-\infty}^{z_r} dz' \exp[U_l(z_r) - U_l(z')] \\ U_l(z) &= (1/D) \left[\frac{(1 + \alpha_l^2)}{\epsilon_i^l} \cdot \text{artg}\left(\frac{z}{\alpha_l}\right) - \frac{\alpha_l^2}{(\epsilon_i^{(l)})^2} \cdot z \right]. \end{aligned} \quad (20)$$

Upon substituting the series expansion $P_l = \sum_k c^k \cdot P_l^{(k)}$, ($l = 0, 1$) in Eq. 19, one obtains an inhomogeneous equation for $P_l^{(k+1)}$, where $P_l^{(k)}$ is the source term. The operator $\mathcal{M}^{(l)}$ is easily inverted, with two integrals over z_r . The integrals are performed numerically. In order to check for convergence, the area difference between successive approximants $P_l^n = \sum_k^n c^k \cdot P_l^{(k)}$ is computed. In the cases exhibited here, we put $c = 0.1$, and find good convergence for $n > 20$.

From the probability distribution $P_l(z)$ we then get $\langle z_r \rangle = \langle z_r \rangle_0 + \langle z_r \rangle_1$, with obvious notation.

In Fig.6 we plot the result $\langle z_r \rangle$ as a function of E_r . The asymptotic behavior in the hermitean case is known: $\langle z_r \rangle \approx (E_r)^{-2}$, ($E_i = 0$) $E_r \gg 1$ [14]. Our estimate,

with $E_i = 10$. and E_r in the range: $50. < E_r < 120.$, is of a much slower decay; further work is needed to clarify this point.

When E_r is fixed, $\langle z_r \rangle$ increases with $|E_i|$, as shown in Fig.7; we get $\langle z_r \rangle \approx |E_i|^\beta$, $\beta \approx 2$ for large enough $|E_i|$.

The value of the wavenumber $\langle z_i(E) \rangle$, emerging in the delocalized regime, can be roughly estimated from $\langle z_r \rangle$ and by choosing, in Eq. 15, the line through the stable point.

It is easily verified that $\langle z_i(E) \rangle$ is an odd function of E_i while $\langle z_r(E) \rangle$ is even; complex conjugate eigenvalues carry opposite wavenumbers. In the hermitean case the two eigenvalues merge, and the wavenumber, being a byproduct of broken parity, is zero for standing waves.

5 Intermediate energies

So far we studied two extreme cases, but intermediate energies in strong disorder can as well be treated; let us consider the following regime: $V_1 \ll E_r \ll V_0$.

The deterministic solutions satisfy Eqs. 8 and 14 respectively, i.e. channel (0) is in a “low energy” regime, and channel (1) in a “high energy” one. The metastable attractor \mathcal{L} is the union of a circle and of a couple of parallel lines. The system for P_0 and P_1 is an hybrid between Eqs. 9 and 19.

The first order operator of Eq. 9 is coupled with the second order one of Eq. 19: this makes an iterative procedure hardly convergent. Based on results from direct numerical integration of Eq. 5, we assign an indeterminacy δ to the circular orbit:

$$\frac{|z|^2}{|\epsilon|^2} = 1 + \delta. \quad (21)$$

An estimate for δ can be extracted [15] from the deterministic flow (see the thickness of the ring in Fig.2). The steady state equation then involves two second order operators:

$$\begin{aligned} \frac{d}{dz_r} [F_r^{(0)} - \frac{d}{dz_r} \mathcal{D}^0] P_0 &= c_1 \cdot P_1 - c_0 \cdot P_0 \\ \frac{d}{dz_r} [A^{(1)} - \frac{d}{dz_r} B^{(1)}] P_1 &= -c_1 \cdot P_1 + c_0 \cdot P_0 \\ \mathcal{D}^0 &= (\delta \cdot |\epsilon^0|^2)^2 \end{aligned} \quad (22)$$

We proceed again by an iterative perturbation scheme. At uncoupled channels ($c = 0$) the “low energy” equation coincides now with the well-known one ([11]), holding in the hermitean case. Its solution carries a non zero probability current: in the present context, it comes from the spread of the circular attractor. The “high energy” integral was already exhibited in the previous section.

In Fig.9 we show the result, the surface $\langle z_r(E) \rangle$. The high energy regime surface is reported for comparison in Fig.8; its contour lines in the E plane are also shown in Fig.10. Qualitative agreement is found with previous numerical and analytical results. An estimate of $\langle z_i(E) \rangle$ can be derived from the adiabatic equations 15 and 8.

6 Conclusions

We studied nonhermitean delocalization in the presence of disordered potentials of Kronig-Penney type, where the barriers have random length. We translated the hamiltonian eigenvalue problem into a stochastic equation for the logarithmic derivative of the wave function ($z = \frac{\psi'}{\psi}$). From the steady state distribution of z we determined the Lyapunov exponent.

Our approach, valid under suitable adiabatic conditions, describes the steady state in terms of the real part of $\langle z \rangle$, an effective wavenumber, can be recovered by means of the adiabatic formulae 8,15.

We analyzed two regimes: a) intermediate energies ($V_1 \ll E_r \ll V_0$); b) high energies ($V_1, V_0 \ll E_r$). The behavior of the system in other regimes is currently under investigation [15].

In case (a), the particle hops in the z plane between a strip and a circle, the strip carrying a probability current. The circle, which acts as a trap for the particle, is absent in case (b), where the 'particle' hops between two strips, with different slopes. Two currents coalesce in this case.

We obtained that $\langle z_r \rangle$ is always decreasing with E_r : at higher energies the wave functions have larger localization length.

At fixed $\langle E_r \rangle$, $\langle z_r \rangle$ increases with $|E_i|$: this means that dissipation (associated with E_i) enhances the localization. The effective wavenumber $\langle z_i \rangle$ increases with E_r , as one would expect with normal dispersion.

The curve $\langle z_r(E) \rangle - a = 0$, a being the convection coefficient, determines the mobility edge in the complex energy plane.

We finally add some comments on the density of states (DOS). Most analytical results on the DOS in the presence of an IMF, possibly with the single exception of the semiclassical analysis by Silvestrov [16], are concerned with the discrete case. Disorder averaging of the resolvent operator can indeed be performed in various discrete models, thus obtaining the DOS in explicit form [7],[8],[9],[10].

The Langevin approach gives the DOS for the hermitean hamiltonian in the continuum. As a preliminary step in that procedure, one writes the definition of the DOS in terms of the z variable: this simply amounts to requiring that $z(x, E)$ must fulfill the boundary condition: $z(L, E) = \bar{z}_L$. This condition is all is needed to determine the DOS, as long as the mapping from E to $z(L, E)$ is invertible, which is precisely the case in the hermitean problem.

Whether anything similar holds in the complex case is, as far as we know, an open question.

References

- [1] N.Hatano,D.R.Nelson:Phys.Rev.Lett.**77**,570(1996).
- [2] J.Miller,Z.J.Wang:Phys.Rev.Lett.**76**,1461(1996).

- [3] J.D.Murray: *Mathematical Biology*, Springer, New York (1993).
- [4] D.R.Nelson,N.M.Shnerb:Phys.Rev.**E58**,1383 (1998).
- [5] N.Hatano,D.R.Nelson:Phys.Rev.**B56**,8651(1997).
- [6] N.Hatano,D.R.Nelson:Phys.Rev.**B58**,8384(1998).
- [7] P.W.Brouwer,P.G.Silvestrov,C.W.J.Beenakker:Phys.Rev.**56**,R4333(1997).
- [8] E.Brezin,A.Zee:Nucl.Phys.**B509**,(1998).
- [9] J.Feinberg,A.Zee:Nucl.Phys.**B504**,579(1997).
- [10] I.Y.Goldsheid,B.A.Khoruzenko:Phys.Rev.Lett.**80**, 2897(1998).
- [11] B.I.Halperin:Phys.Rev.**139**,A104(1965).
- [12] M.M.Benderskii,L.A.Pastur: *JETP* **57**,284(1969).
- [13] B.Souillard in:"Chance and Matter", J.Souletie,J.Vannimenus, R.Stora editors,North Holland,(1987).
- [14] I.M.Lifshits,S.A.Gredeskul,L.A.Pastur:"Introduction to the theory of disordered systems",Wiley,New York,(1988).
- [15] V.G.Benza,S.Manildo, in preparation.
- [16] P.G.Silvestrov:Phys.Rev.**58**,R10111(1998).

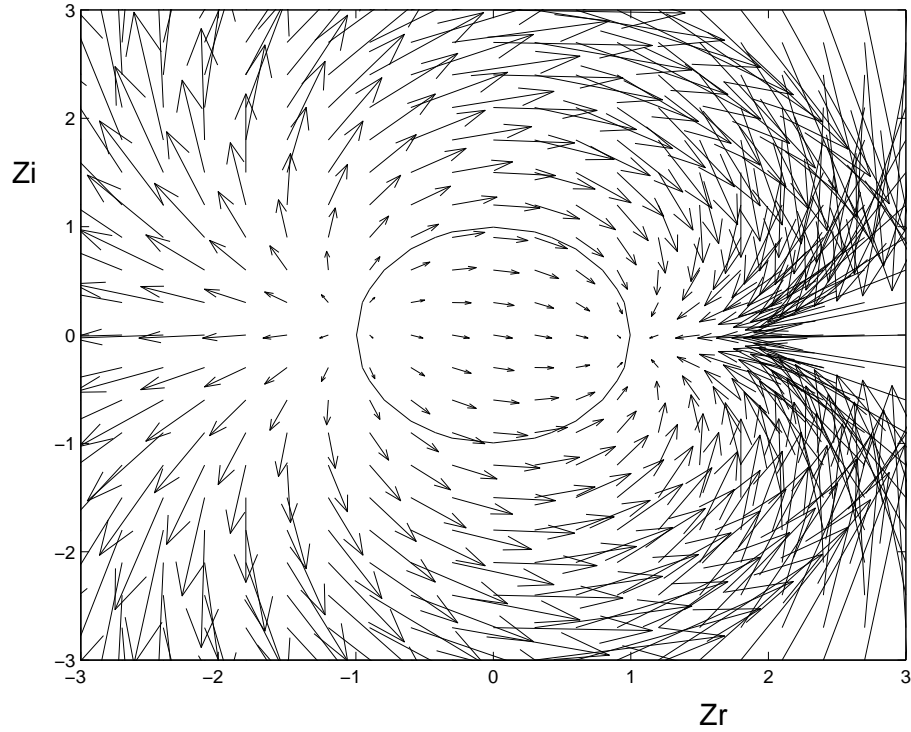


Fig.1: Vector field (F_r, F_i) in the z plane for the Equation 5 at fixed $s(x)$ (deterministic), in the low energy regime. The variables z_r, z_i are in arbitrary units of $(length)^{-1}$. The superimposed circle corresponds to the metastable attractor discussed in the text (see Eq. 8). The two critical points characterized by the condition $F_r = 0, F_i = 0$ belong to the circle.

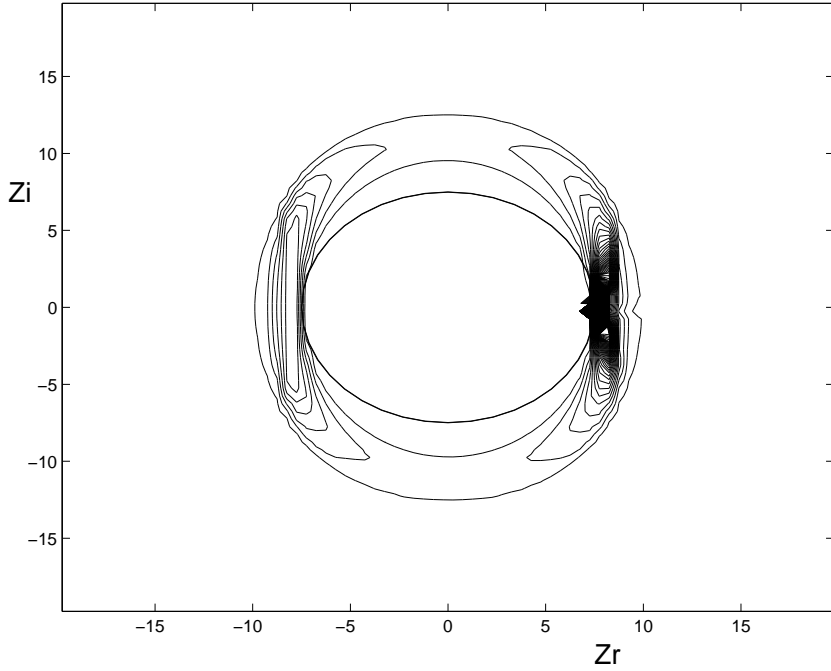


Fig.2:Numerical integration of the Equation 5 with $s(x) = 0$ in the low energy regime: contour lines of the probability distribution at an intermediate time. The variables z_r, z_i are in arbitrary units of $(length)^{-1}$. The distribution is obtained from 2000 random initial conditions. The inner circle is superimposed: it corresponds to the metastable attractor, as calculated from Eq. 8, with the values $E_r - V_0 = -56, E_i = -1.35$ used in the numerical integration. The variables E_r, E_i are in arbitrary units of $(length)^{-2}$. The unstable critical point is on the left of the ring; the peak at the stable point can be seen on the right. The distribution deviates from a purely circular behavior; it is elongated in the aequator direction, if one takes the critical points as the poles. In fact going from the low to the high energy regime (see Eq.15) the attractor is converted into a couple of lines. These lines are through the poles, and parallel to the aequator.

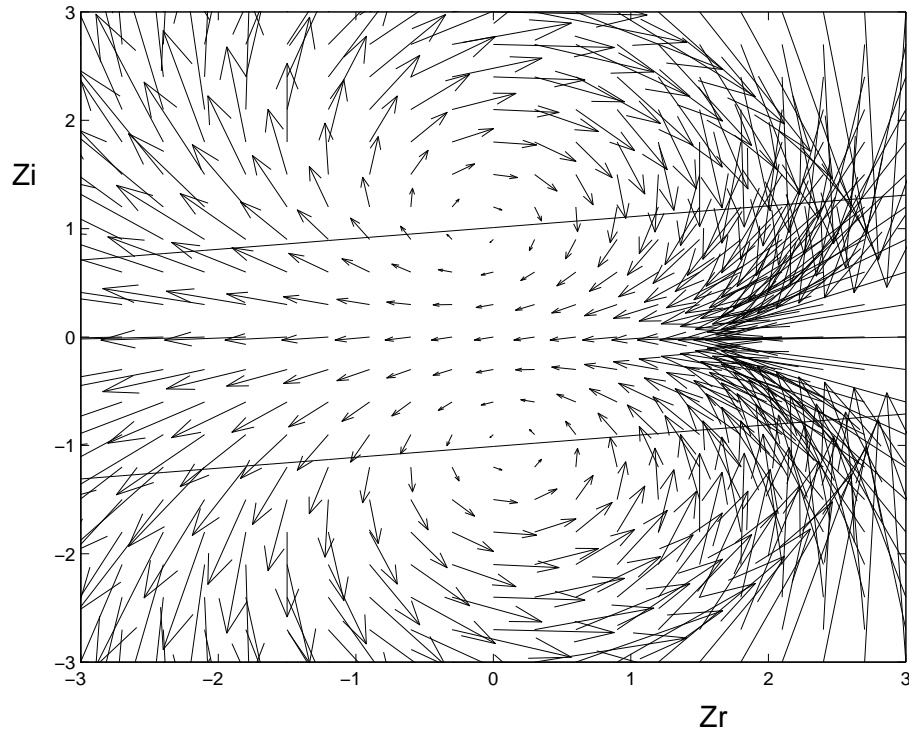


Fig.3: Vector field (F_r, F_i) of Equation 5 with fixed $s(x)$ in the high energy regime. The variables z_r, z_i are in arbitrary units of $(length)^{-1}$. The two superimposed parallel lines through the critical points $(F_r = 0, F_i = 0)$ correspond to the metastable attractor (see Eq. 15). The lines are orthogonal to the segment connecting the critical points.

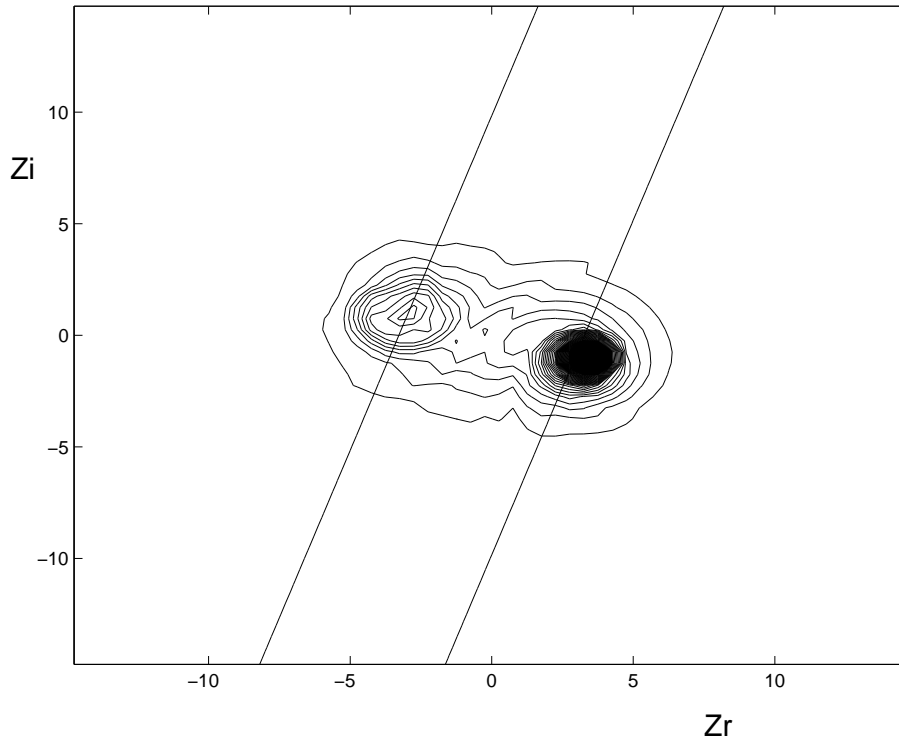


Fig.4:Numerical integration of Eq. 5 with $s(x) = 1$ in the high energy regime (random initial conditions): contour lines of the probability distribution at an intermediate time. The variables z_r, z_i are in arbitrary units of $(length)^{-1}$. The energy values are $E_r - V_1 = 10.35$, $E_i = 7.5$, in arbitrary units of $(length)^{-2}$. The unstable critical point is in the upper left. The metastable attractor (two parallel lines) has been superimposed; with respect to Fig.3, we are here at lower energies (the critical points are closer to the axis z_r). One can notice, in particular around the unstable point, that the distribution is slightly elongated in the direction of the attractor.

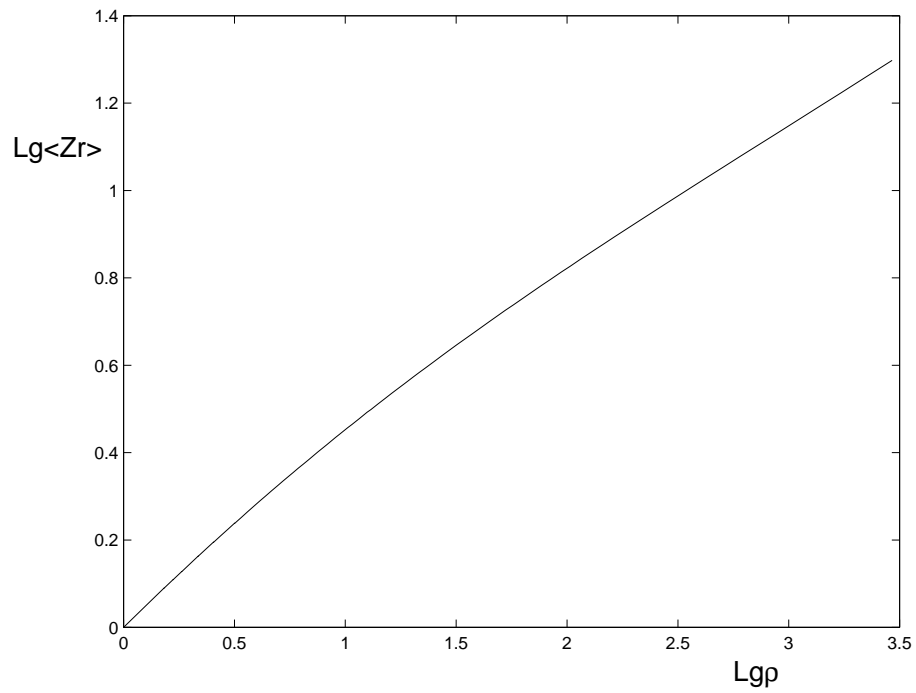


Fig.5: Low energy regime; from the solution (Eq. 11) of the steady state Equation 9 for the probability: log-log plot of $\langle z_r \rangle$ versus $\rho = \frac{\epsilon_i^{(0)}}{\epsilon_i^{(1)}}$. Higher ρ means higher disorder (see text): the localization length decreases with ρ .

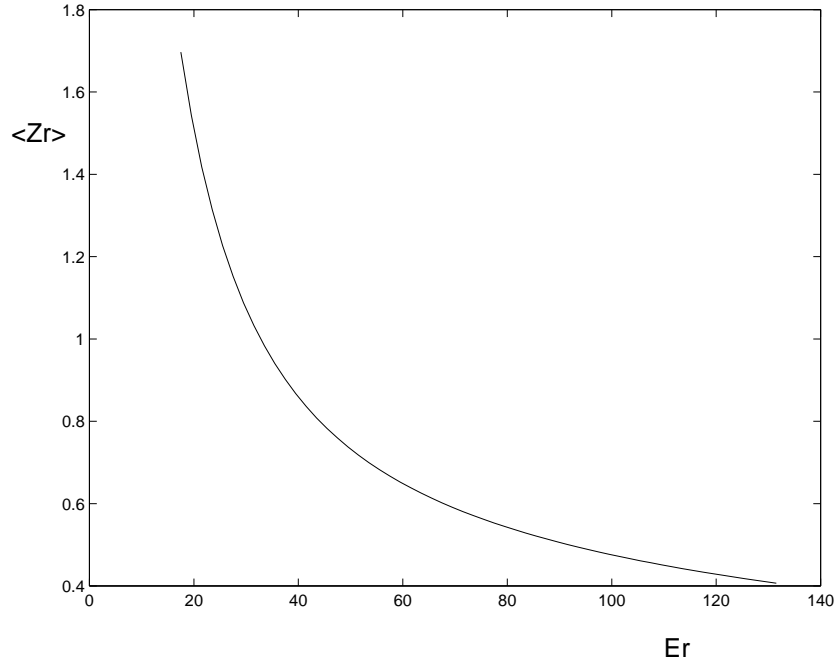


Fig.6: High energy regime: $\langle z_r \rangle$ versus E_r at fixed E_i , ($E_i = 10$). The variable z_r is in arbitrary units of $(length)^{-1}$, and E in arbitrary units of $(length)^{-2}$. The origin of the energy axis corresponds to $E_r = \frac{1}{2} \cdot (V_{(0)} + V_{(1)})$; $V_{(0)} - V_{(1)} = 5$. From numerical integration of the probability Equation19 at steady state, with $D = 0.1$. The regularization parameter is: $\xi^{(l)} = \epsilon_i^l$. With this choice $\xi^{(l)}$ has the same order of magnitude of z_r at the stationary points: $z_r = \pm \epsilon_i^{(l)}$.

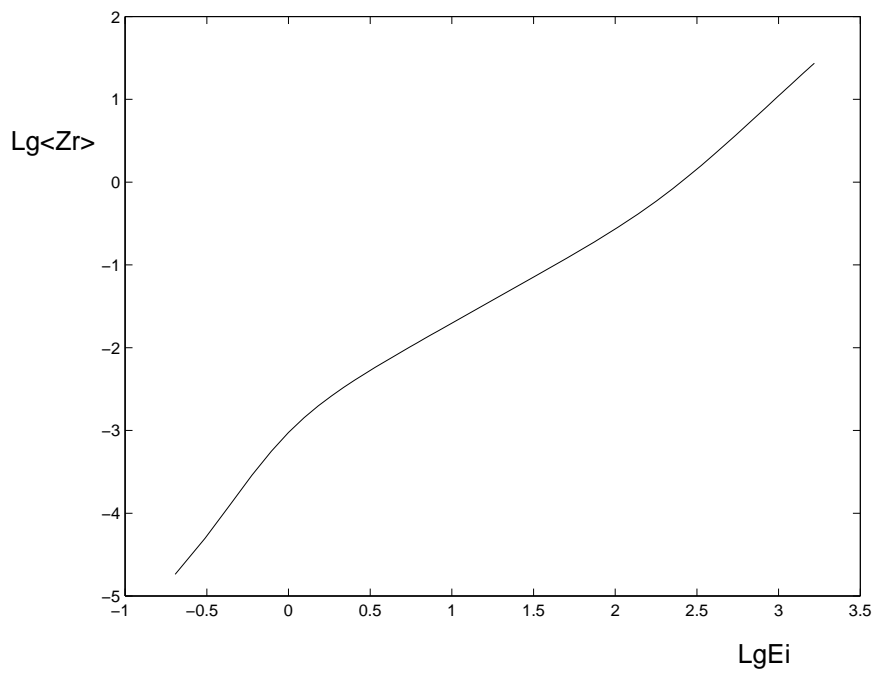


Fig.7: High energy regime: log-log plot of $\langle z_r \rangle$ versus E_i at fixed E_r : $E_r - V_{(1)} = 60.$, $E_r - V_{(0)} = 30$. Same Equation and parameters as in Fig.6.

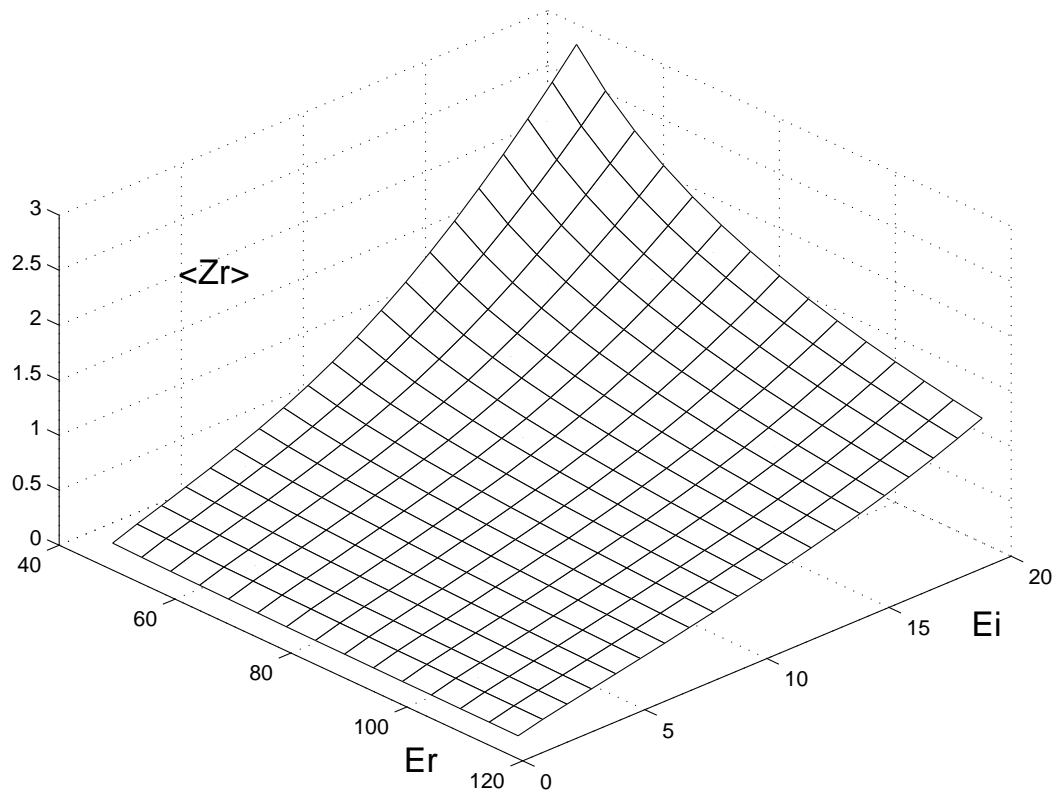


Fig.8: High energy regime:global behavior of $\langle z_r \rangle$ versus E ; $V_{(0)} - V_{(1)} = 30$. The variable z_r is in arbitrary units of $(length)^{-1}$, and E in arbitrary units of $(length)^{-2}$. From numerical integration of Equation 19 for the steady state probability. Same parameters as in Figs. 6,7.

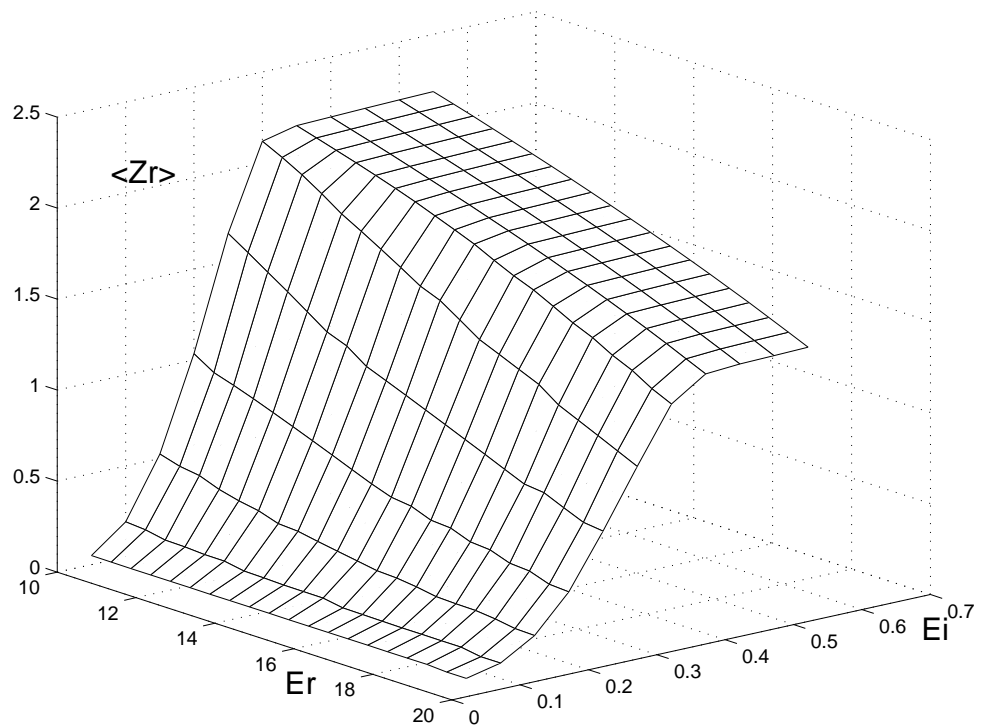


Fig.9: Intermediate energy regime, from numerical integration of the Equation 22 for the steady state probability: $\langle z_r \rangle$ versus $E, D = 0.1, \delta = 25., V_{(0)} - V_{(1)} = 30$. The variable z_r is in arbitrary units of $(length)^{-1}$, and E in arbitrary units of $(length)^{-2}$.

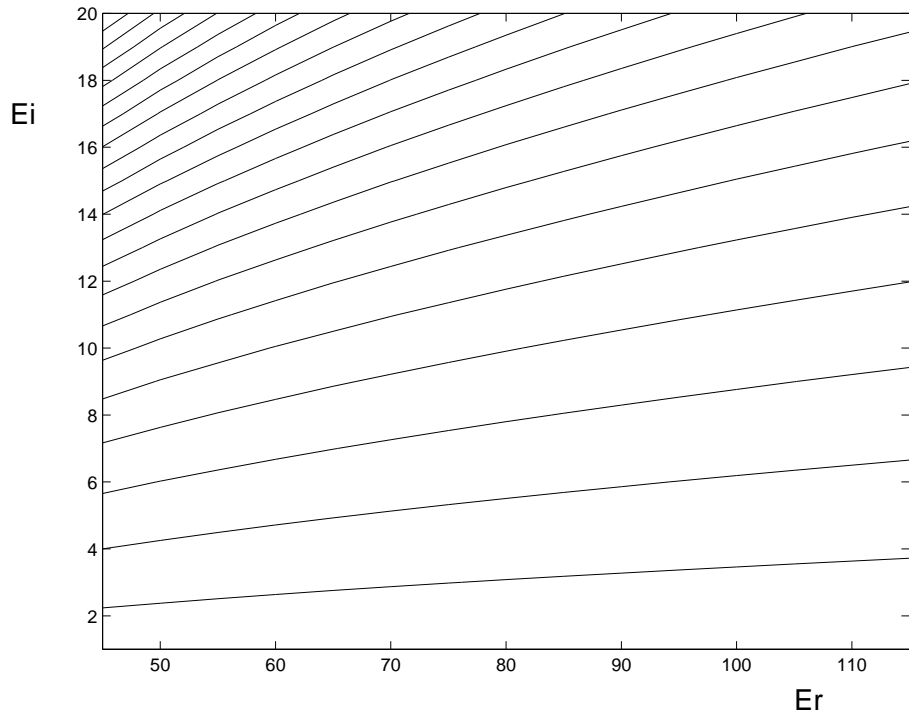


Fig.10:High energy regime.Contour lines of the surface $\langle z_r(E) \rangle$ plotted in Fig.8. E_r , E_i are in arbitrary units of $(length)^{-2}$. Each line identifies a mobility edge, for a given convection parameter a ; a increases from bottom right to top left, in a range of values from 0.1 to 2.95, with step 0.15.